Adv. Polar Upper Atmos. Res., **13**, 154–161, 1999

DETECTION OF THE ONSET TIME OF Pi 2 PULSATIONS BY USING WAVELET ANALYSIS

Kayoko TSUNEZAWA[1], Yutaka TONEGAWA[1] and Tohru SAKURAI[1]

[1] *Tokai University, 1117 Kitakaname, Hiratsuka 259-1292*

Abstract: We have developed an algorithm for automatic detection of the onset of Pi 2 pulsations by using the wavelet transform. It is found that the Cauchy wavelet with proper parameters has a time resolution higher than that of the Gabor wavelet, and is suitable for detecting Pi 2 onset. It is revealed that the time of power peak of the Cauchy wavelet transform is given within one to three minutes after the onset of Pi 2. This time lag has been automatically compensated in the present algorithm, and it is shown that the onset time of almost all Pi 2 events can be determined with an accuracy of one minute.

1. Introduction

It is well known that Pi 2 magnetic pulsations occur at the onset of every individual magnetic storm. SAKURAI and SAITO (1976) examined the coincidence between the onset of sudden brightening of the auroral arc in the auroral oval and the onset of Pi 2 at low latitudes. They concluded that the onset of substorms can be identified quite well with the onset of Pi 2. Nowadays, it is very popular to determine the onset time of substorm by the onset of Pi 2.

The onset time of Pi 2 has been determined by visual inspection of magnetograms for many years. NOSE *et al.* (1998) have recently developed an algorithm to detect the Pi 2 envelope and its onset time by using a wavelet analysis. They showed that in 90.8 % (97.9%) of Pi 2 events the onset time determined by their algorithm detection coincide with that identified by the visual detection, with an accuracy of ± 1 min (± 2 min). They have used the Mayer wavelet as a mother wavelet, and simply defined the onset of Pi 2 as the time when the wavelet coefficient exceeds a certain threshold value. In order to detect the onset of Pi 2 more accurately, we try different kinds of mother wavelet and more sophisticated algorithms in this study.

2. Wavelet Analysis

A recently developed mathematical technique, wavelet analysis, can be used to represent functions that are local in time and frequency (MORLET *et al.*, 1982). The wavelet analysis is a suitable method for investigating the wave characteristics of phenomena which are limited in both time and frequency, such as Pi 2 pulsations. The wavelet transform of the time series $f(t)$ is defined as

$$(W_\phi f)\ (a,b)=\frac{1}{\sqrt{a}}\int_{-\infty}^{\infty} f(t)\ \phi\left(\frac{t-b}{a}\right)\mathrm{d}t, \tag{1}$$

where $\phi(t)$ is the basic wavelet (or a "mother wavelet") with effective length that is usually much shorter than the target time series $f(t)$. The variables are a and b: a is the dilation/compression scale factor that determines the characteristic frequency so that varying a gives rise to a "spectrum"; and b is the translation in time so that varying b represents the "sliding" of the wavelet over $f(t)$. The wavelet spectrum is thus customarily displayed in the time-frequency domain, or the $a-b$ space with the horizontal time axis b and the vertical frequency axis a. Orthogonal sets of $\phi(t-b)/a$ (when a varies in powers of 2 or an "octave") are often exploited in applications involving inverse transforms and the reconstruction of signals.

For our application we select the Gabor wavelet and the Cauchy wavelet as a mother wavelet. The Gabor wavelet is used commonly for the Continuous Wavelet Transform, and it is suited for searching the frequency of signals (CHUI, 1992). It is given by

$$\phi(t)=\frac{1}{2\sqrt{\pi}\,\sigma}\ e^{-\frac{t^2}{\sigma^2}}e^{-it}, \tag{2}$$

where σ is the width of the Gaussian envelope. The time and frequency resolutions of the Gabor wavelet transform depend on the magnitude of σ. A smaller σ gives higher time resolution but lower frequency resolution. We have tried several values of σ, and found $\sigma=8$ is suitable for Pi 2 pulsations, so we use this value in our analysis.

On the other hand, the Cauchy wavelet (HOLSCHNEIDER, 1995) is not so popular, although the shape of this mother wavelet is similar to that of Pi 2 pulsation. The Cauchy wavelet is given by

$$\phi(t)=(2\pi)^{-1}\Gamma\ (\gamma+1+i\beta)\ (1-it)^{-(1+\gamma+i\beta)},\ \gamma>0, \tag{3}$$

where Γ is a Gamma function, and γ, β are parameters of the mother wavelet. The waveform of $\phi(t)$ with $\gamma=2$~4 and $\beta=3$~7 can be well similar to Pi 2 pulsations. In this study, we use the set of $\gamma=3$ and $\beta=5$, because we have found it to be one of the best parameter set for our algorithm that will be discussed in Section 4. The upper and lower panels in Fig. 1 show waveforms of the Gabor and Cauchy wavelets, respectively.

3. Example of Wavelet Analysis

In this study we use the geomagnetic field data observed by a fluxgate magnetometer at Tokai University Space Information Center at Kumamoto (22.5°N geomagnetic latitude, 199.7° E geomagnetic longitude) in October 1996 (SAKATA *et al.*, 1998). The magnetic field sampling with 1 s is differentiated with respect to time, and then treated with the running average of 20 s in advance of analysis.

The H differentiated component ($\mathrm{d}H/\mathrm{d}t$) observed in the period of 1400–1500 UT

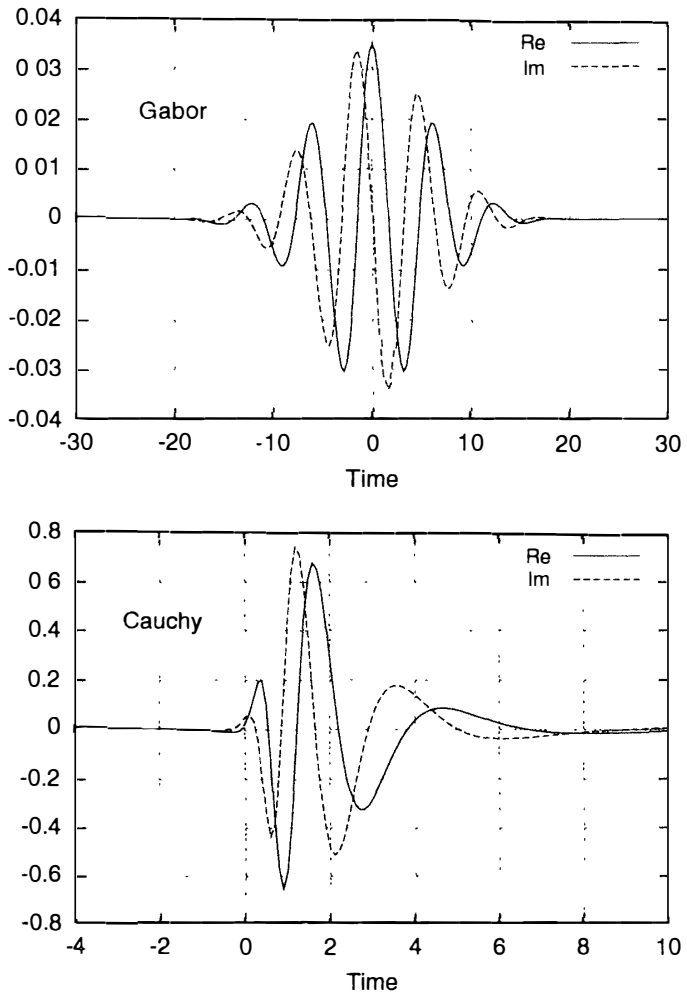

Fig. 1. Waveforms of the Gabor wavelet (upper panel) and the Cauchy wavelet (lower panel). Solid and dashed curves show the real and imaginary parts, respectively.

on October 10, 1996 is plotted in the bottom panel of Fig. 2. Three Pi 2 pulsations were excited at 1419, 1433, and 1443 UT. The top and middle panels show the corresponding dynamic (time-frequency) spectra of Gabor and Cauchy wavelets, respectively. Both of the wavelet analyses are well demonstrated that they are useful methods for analyzing characteristics of Pi 2 pulsations in the time-frequency domain. Enhancements of spectral power corresponding to the Pi 2s are clearly detected in the both dynamic spectra. Horizontal and vertical lines in the dynamic spectra indicate the positions of spectral peaks in the frequency and time domains, respectively. Spectral peaks of Gabor and Cauchy are obtained at slightly different positions. For example, the spectral peak of the first Pi 2 is at 16.6 Hz, 1421:36 UT for Gabor, and 18.2 Hz, 1420:48 UT for Cauchy. It is shown that the Cauchy spectrum is broad in the frequency domain rather than Gabor one, *i.e.* lower frequency-resolution. However, the Cauchy wavelet shows a higher time-resolution, and its spectral peaks are located close to the actual onset times of Pi 2s rather than those of Gabor. Therefore, we apply

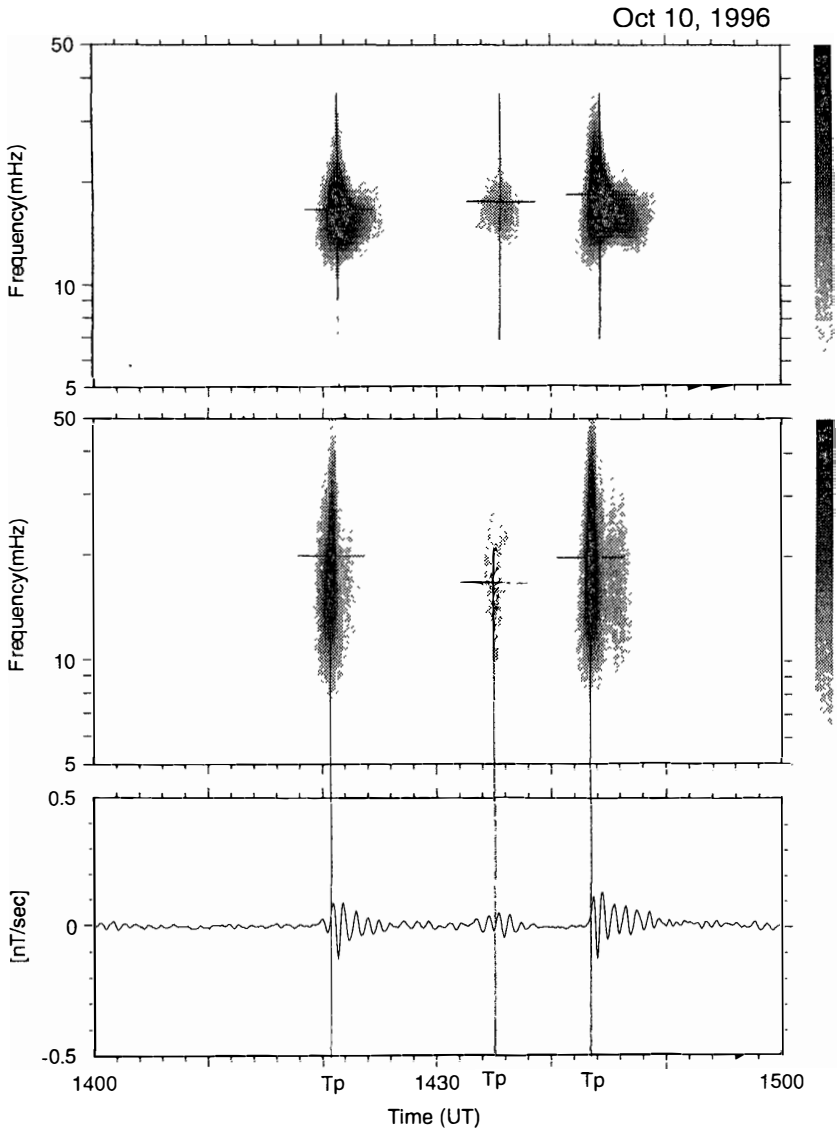

Fig. 2. Dynamic spectra calculated by using the Gabor wavelet (top panel) and the Cauchy wavelet (middle panel), and corresponding waveform of Pi 2 pulsations (bottom panel) observed at Kumamoto in the period of 1400–1500 UT on October 10, 1996.

the Cauchy wavelet to an automated detection of Pi 2 onset time.

4. Algorithm for Detecting Pi 2 Onset Time

As the first step to determine the onset time of Pi 2s, we look for the time of spectral peak in the dynamic spectrum of the Cauchy wavelet transform. Figure 3 shows an expanded waveform of the dH/dt component for the same interval of Fig. 2. Vertical dotted lines in Fig. 3 represent the times of the spectral peak, T_P. Arrows indicate the actual onsets of Pi 2, which was determined by visual inspection. As shown in this

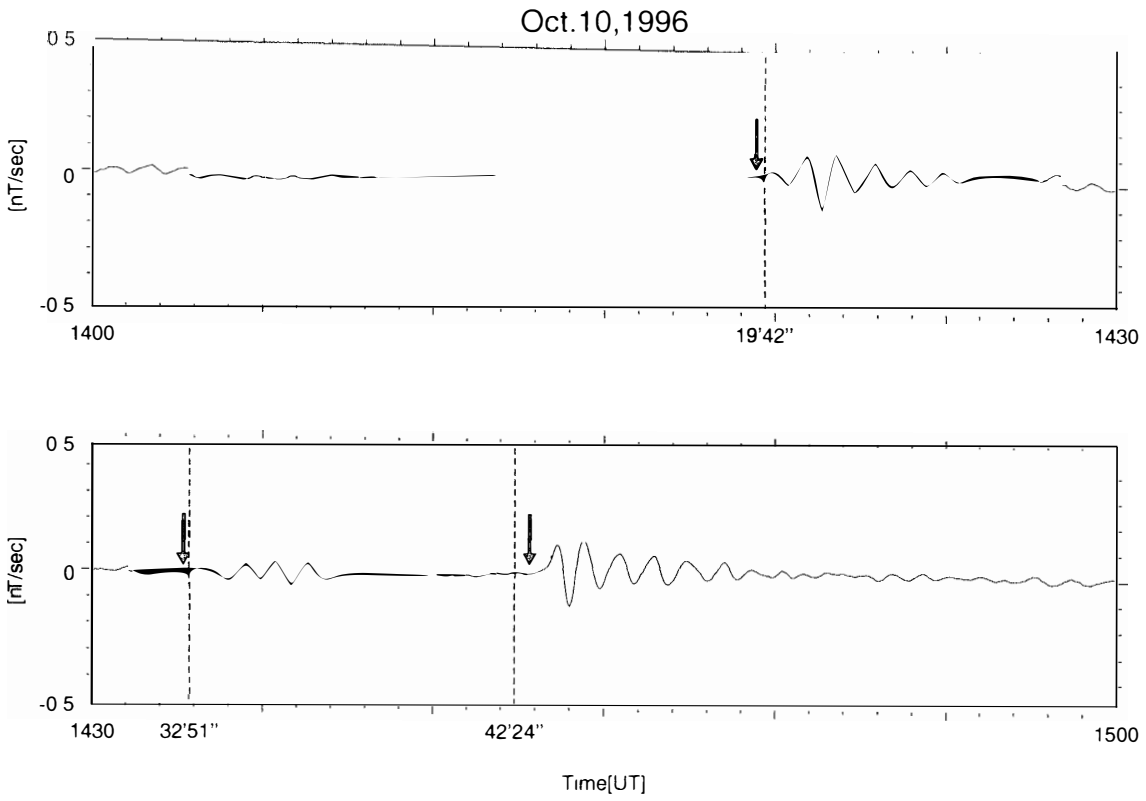

Fig. 3. A plot of the H differentiated component in the same interval of Fig. 2. Vertical dotted lines show the times of the spectral peaks (T_P). Dashed lines represent the onset time of Pi 2s detected by the algorithm shown in Fig. 4. Arrows indicate the onset time based on visual judgment.

figure, the spectral peaks are obtained behind the actual onsets. We have checked all Pi 2 events observed at Kumamoto in October 1996, and found that the spectral peaks corresponding to Pi 2s lagged 1–3 min behind the actual onset time. There was no case of the spectral peak earlier than the actual onset, when we used the parameters of $\gamma=3$ and $\beta=5$ for the Cauchy wavelet. This is the reason why we choose this parameter set for our algorithm in which the spectral peak, T_P, must come after the onset of Pi 2.

The next step is to logically determine a commencement time of the excited Pi 2 wave, *i.e.* the onset time. We define the onset time as the first zero-crossing point on the Pi 2 waveform of the dH/dt component. This definition is generally suitable for the time-differentiated data with the base line of zero. However, the first zero-crossing method is unusable when the data have some bias such as Pi 2 events observed with a long-duration magnetic variation, *e.g.*, a positive bay of the H component. In order to remove the bias, the averaging value for 20 min before and after the Pi 2 is subtracted from dH/dt data in advance of the following process.

The upper part of Fig. 4 shows a schematic Pi 2 waveform and time marks of, T_P, T_1, T_2 and T_0, which are used in the process to determine the onset time. T_P is the time of spectral peak, and it always lags behind the actual onset time. T_1 and T_2 are times of the two adjacent peaks of the oscillation, and $T_1<T_2$. The time of zero crossing

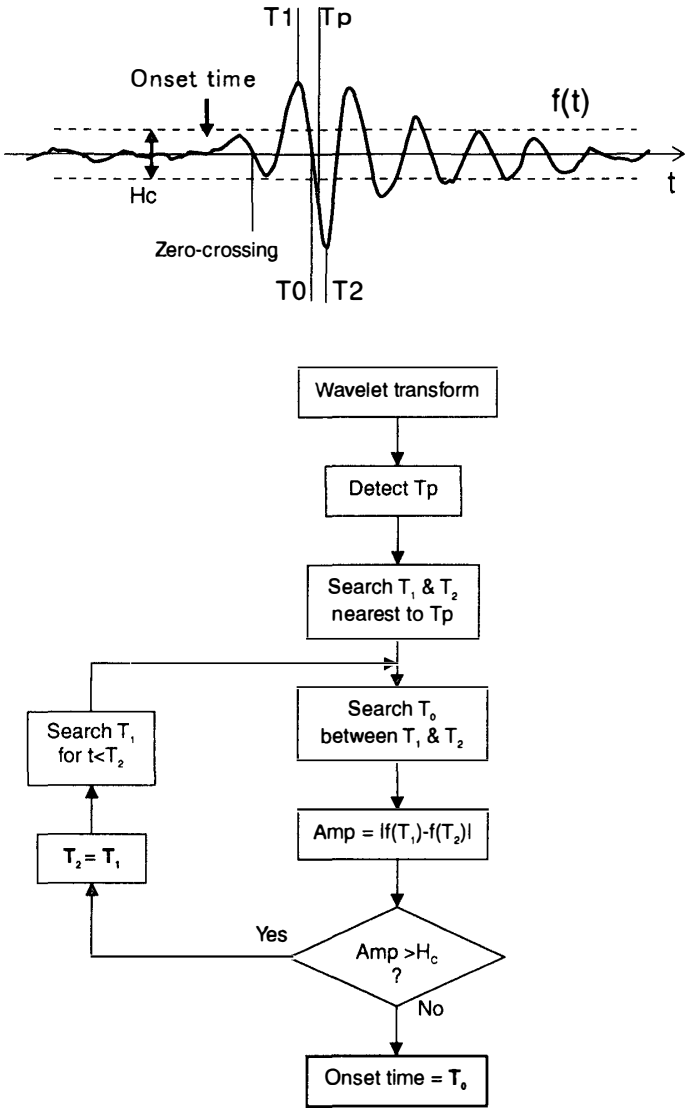

Fig. 4. A schematic Pi 2 waveform and a flowchart of the algorithm to detect the onset time of Pi 2. T_P is the time of spectral peak. T_1 and T_2 are times of two adjacent peaks of the oscillation, and $T_1 < T_2$. T_0 is the time of zero crossing between T_1 and T_2.

between T_1 and T_2 is referred to T_0. At first, those of T_1, T_2, and T_0 nearest to T_P are found, and then they are searched again for earlier wave peaks successively until the wave amplitude, $|f(T_1)-f(T_2)|$, reduces to a value smaller than the threshold of H_C. This minimum amplitude threshold has been set empirically as $H_C=0.043$ nT/s. In this process, we take the final T_0 as the onset time of Pi 2. The flowchart of this algorithm is shown in the lower part of Fig. 4.

Dashed lines in Fig. 3 represent the onset times detected by the algorithm. It is shown that the onset times detected automatically are well coincident with those identified by visual inspection. For the three Pi 2 events in Fig. 3, the time differences

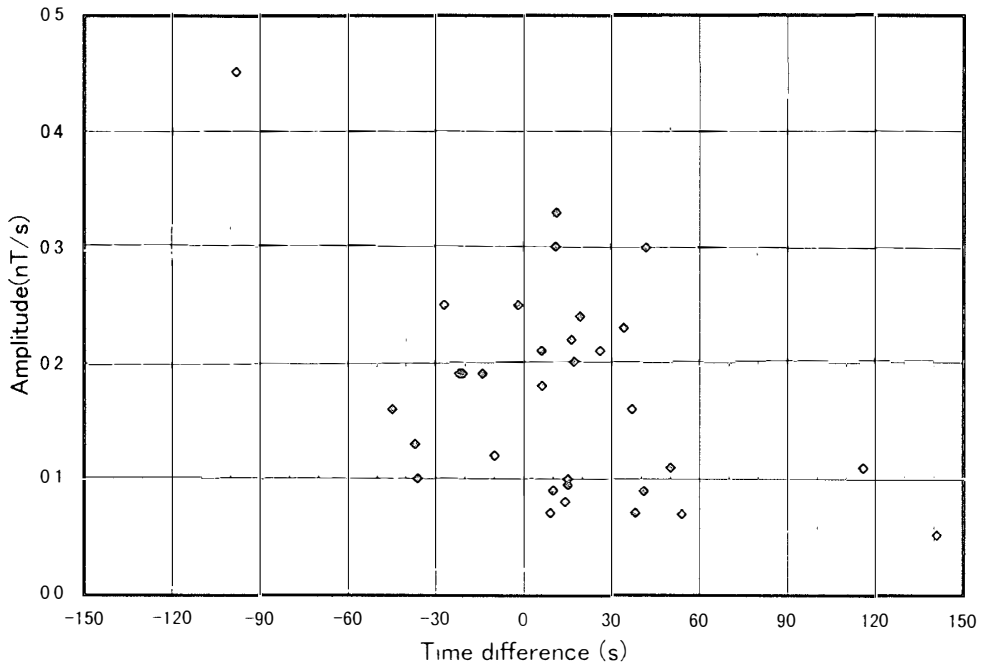

Fig. 5. Distribution of time differences between the onsets determined by the algorithm and visual decision. A positive time difference denotes a time lag of the algorithm detection behind the visual one. The ordinate is the amplitude of each Pi 2 wave.

between the visual and algorithm detection are 16 s, 10 s, and 27 s, respectively.

We have found 32 relatively isolated Pi 2 events in October 1996, and we applied the algorithm detection of the onset for all of these events. The result is shown in Fig. 5, which plots the time differences between onsets determined by the algorithm and visual detection, against the maximum amplitude of each Pi 2 wave. A positive difference indicates that the onset determined by the algorithm detection lags behind that of visual detection. The average of the onset time differences is +13 s, and in 91 % (59%) of the events the onset time detected by the algorithm coincides with that determined by the visual detection with an accuracy of ±60 s (±30 s). The figure also shows that there is no tendency for the time difference to depend on the Pi 2 amplitude, and that the accuracy is maintained even if the amplitude is small.

There are only three events for which the time difference is larger than one minute. For the two events, the time detected by the algorithm is much behind the visual onset time. Waveforms of these Pi 2s are not typical damping oscillations and their amplitudes are relatively small. It may be also difficult to define the exact onset time visually for these cases. The other large error of −98 s has been caused for the largest Pi 2 event. This Pi 2 wave is a clear damping oscillation, however the waveform with the large amplitude of 0.45 nT/s is not symmetric along the time axis. Therefore, the bias still remained after the time averaging was subtracted, and the first zero crossing, could not be detected properly. We have tried several band-pass filters to remove this kind of bias, however the result was unsatisfactory for our algorithm because of additional artificial oscillations caused by the numerical filter.

5. Summary

In this study we have aimed at developing an algorithm for an objective determination of Pi 2 onset time by using the wavelet transform. Characteristics of the wavelet transform depend much on the choice of a mother wavelet. The Gabor and Cauchy wavelets have been examined for detecting the onset time of Pi 2. It was shown that the Cauchy wavelet has a higher time-resolution, and its spectral peak is located closer to the actual onset of Pi 2 than the Gabor wavelet. In order to realize this advantage for the Cauchy wavelet, we have found suitable parameters ($\gamma=3$ and $\beta=5$) for the mother wavelet. Furthermore, we have introduced an algorithm in which we simulated the process of the visual detection of the onset time. We applied this algorithm to Pi 2 events observed at Kumamoto in December 1996. The result showed that the present algorithm could determine the onset time with an accuracy of ± 60 s (± 30 s) for 29 (19) cases out of 32 Pi 2 events. There are only three cases whose errors are more than one minute, and what causes these errors has been revealed in the previous session. It might be emphasized that our algorithm has a possibility to determine the onset time with the accuracy of one minute for all Pi 2 pulsations of which onset time can be clearly identified.

Acknowledgments

We would like to express our appreciation for receiving the guidance and encouragement from Prof. T. SAKATA, Director of the Tokai Space Information Center (TSIC). We also acknowledge to Dr. H. YOKOTSUKA and Mr. K. SAKATA for their help with the data processing. The work presented in this paper was supported by the Tokai University Research and Information Center (TRIC) and National Institute of Polar Research (NIPR).

References

CHUI, C.K. (1992): An Introduction to Wavelets. Boston, Academic Press, 264p.

HOLSCHNEIDER, M. (1995): Wavelets an Analysis Tool. New York, Oxford University Press, 35–36.

MORLET, J., AREHS, G., FOURGEAU, I. and GIARD, D. (1982): Wave propagation and sampling theory. Geophysics, **47**, 203.

NOSE, M., IYEMORI, T., TAKEDA, M., KAMEI, T., MILLING, D.K., ORR, D., SINGER, H.J., WORTHINGTON, E. W. and SUMITOMO, N. (1998): Automated detection of Pi 2 pulsations using wavelet analysis: 1. Method and an application for substorm monitoring. Earth Planets Space, **50**, 773–783.

SAKATA, K., TONEGAWA, Y., SAKURAI, T. and YOKOTSUKA, H. (1998): Development of geomagnetic field observation system at the Tokai university. Proc. Sch. Eng. Tokai Univ., **38**, 231–237.

SAKURAI, T. and SAITO, T. (1976): Magnetic pulsation Pi2 and substorm onset. Planet. Space Sci., **24**, 573–575.

(Received January 18, 1999; Revised manuscript accepted May 19, 1999)